



Gravitational footprints of massive neutrinos and lepton number breaking

Andrea Addazi ^{a,b}, Antonino Marcianò ^{a,g}, António P. Morais ^{c,*}, Roman Pasechnik ^d, Rahul Srivastava ^{e,f}, José W.F. Valle ^e

^a Department of Physics & Center for Field Theory and Particle Physics, Fudan University, 200433 Shanghai, China

^b College of Physics, Sichuan University, Chengdu, 610065, China

^c Departamento de Física, Universidade de Aveiro and CIDMA, Campus de Santiago, 3810-183 Aveiro, Portugal

^d Department of Astronomy and Theoretical Physics, Lund University, 221 00 Lund, Sweden

^e AHEP Group, Institut de Física Corpuscular – C.S.I.C./Universitat de València, Parc Científic de Paterna. C/ Catedrático José Beltrán, 2 E-46980 Paterna (Valencia), Spain

^f Department of Physics, Indian Institute of Science Education and Research - Bhopal, 462066 Madhya Pradesh, India

^g Laboratori Nazionali di Frascati INFN, 00044 Frascati - Rome, Italy



ARTICLE INFO

Article history:

Received 17 October 2019

Received in revised form 15 April 2020

Accepted 9 June 2020

Available online 25 June 2020

Editor: G.F. Giudice

ABSTRACT

We investigate the production of primordial Gravitational Waves (GWs) arising from First Order Phase Transitions (FOPTs) associated to neutrino mass generation in the context of type-I and inverse seesaw schemes. We examine both “high-scale” as well as “low-scale” variants, with either explicit or spontaneously broken lepton number symmetry $U(1)_L$ in the neutrino sector. In the latter case, a pseudo-Goldstone majoron-like boson may provide a candidate for cosmological dark matter. We find that schemes with softly-broken $U(1)_L$ and with single Higgs-doublet scalar sector lead to either no FOPTs or too weak FOPTs, precluding the detectability of GWs in present or near future measurements. Nevertheless, we found that, in the majoron-like seesaw scheme with spontaneously broken $U(1)_L$ at finite temperatures, one can have strong FOPTs and non-trivial primordial GW spectra which can fall well within the frequency and amplitude sensitivity of upcoming experiments, including LISA, BBO and u-DECIGO. However, GWs observability clashes with invisible Higgs decay constraints from the LHC. A simple and consistent fix is to assume the majoron-like mass to lie above the Higgs-decay kinematical threshold. We also found that the majoron-like variant of the low-scale seesaw mechanism implies a different GW spectrum than the one expected in the high-scale seesaw. This feature will be testable in future experiments. Our analysis shows that GWs can provide a new and complementary portal to test the neutrino mass generation mechanism.

© 2020 The Authors. Published by Elsevier B.V. This is an open access article under the CC BY license (<http://creativecommons.org/licenses/by/4.0/>). Funded by SCOAP³.

1. Introduction

Non-zero neutrino masses constitute one of the most robust evidences for new physics [1–3]. Despite great efforts over the last two decades to underpin the origin of neutrino mass, the basic underlying mechanism remains as elusive as ever. Small neutrino masses can be generated in many ways, both for Majorana [4,5] and Dirac [6–11] neutrinos. Here, we focus on the various variants of the popular type-I seesaw mechanism for Majorana neutrinos [12–15]. We consider both high- and low-scale [16–20] re-

alizations, with explicit or spontaneous lepton number violation, in which $SU(3)_C \otimes SU(2)_L \otimes U(1)_Y$ singlet neutrinos act as neutrino mass mediators. Besides oscillation and neutrinoless double beta decay ($0\nu 2\beta$) searches, neutrino masses can be probed through Charged Lepton Flavor Violation (CLFV) experiments at the high intensity and/or high energy frontier [21–23]. Moreover, neutrino mass generation can leave signatures at high-energy colliders like the Large Hadron Collider (LHC) [24–27].

The detection of Gravitational Waves (GWs) by the LIGO team has opened an entirely novel method to probe the underlying new physics associated to neutrino mass generation. It was advocated that the spectrum of primordial GWs, potentially measurable at the currently planned GW interferometers, may represent an important cutting-edge probe for new physics. This follows from the fact that these interferometers can be sensitive enough to

* Corresponding author.

E-mail addresses: andrea.addazi@lngs.infn.it (A. Addazi), marciano@fudan.edu.cn (A. Marcianò), aapmorais@ua.pt (A.P. Morais), Roman.Pasechnik@hep.lu.se (R. Pasechnik), rahul@iiserb.ac.in (R. Srivastava), valle@ific.uv.es (J.W.F. Valle).

measure the echoes of the possible First Order Phase Transitions (FOPTs), which might have happened in the past cosmological history [28].

In this letter, we focus on possible gravitational footprints of the various variants of the popular type-I and inverse seesaw mechanisms for Majorana neutrinos. The relevant part of the minimal type-I seesaw Lagrangian is given by

$$\mathcal{L}_{\text{Yuk}}^{\text{Type-I}} = Y_\nu \bar{L} H \nu^c + M \nu^c \nu^c + \text{h.c.} \quad (1)$$

Here, $L = (\nu, l)^T$ are the SM lepton doublets, H is the SM Higgs doublet, ν^c are the three SM singlet “right-handed” neutrinos. The 3×3 matrices Y_ν and M are the Yukawa coupling and the ν^c mass matrix, respectively. Due to the Pauli principle the latter is symmetric. Notice that, for brevity, we omit family indices throughout this letter. Notice also that the mass term explicitly breaks the lepton number symmetry $U(1)_L$ to its \mathbb{Z}_2 subgroup. The electroweak (EW) symmetry is broken by the vacuum expectation value (vev) of the Higgs field, i.e. $\langle H \rangle = v_h/\sqrt{2}$, generating the light neutrino masses

$$m_\nu^{\text{Type-I}} = \frac{v_h^2}{2} Y_\nu^T M^{-1} Y_\nu. \quad (2)$$

The lightness of the left-handed neutrinos is then ascribed to the heaviness of the “right-handed” isosinglet partners e.g. for $Y \sim \mathcal{O}(1)$, $M \sim \mathcal{O}(10^{14})$ GeV, one gets $m_\nu \sim \mathcal{O}(0.1)$ eV.

Another popular realization of this idea is the “low-scale” variant, in which two gauge singlet fermions ν^c and S are added sequentially to the SM particle content [16–20]. The template of these schemes has exact conservation of lepton number and, as a result, strictly massless neutrinos. Yet flavor is violated to a potentially large degree, subjected only to constraints from weak interaction precision observables, such as universality tests [29–33]. To this template one adds a small seed of lepton number violation, leading to nonzero neutrino mass. One example is the so-called “inverse seesaw” mechanism, where the smallness of the neutrino mass is linked to the breaking of the lepton number symmetry $U(1)_L$ to its \mathbb{Z}_2 subgroup, through the so called μ -term. The relevant part of Lagrangian in this case is given by

$$\mathcal{L}_{\text{Yuk}}^{\text{Inverse}} = Y_\nu \bar{L} H \nu^c + M \nu^c S + \mu S S + \text{h.c.}, \quad (3)$$

where μ is also a 3×3 symmetric matrix. The light neutrino mass is then given by

$$m_\nu^{\text{Inverse}} = \frac{v_h^2}{2} Y_\nu^T M^{T^{-1}} \mu M^{-1} Y_\nu. \quad (4)$$

Note that small neutrino masses are “protected”, since $m_\nu \rightarrow 0$ as the lepton number symmetry gets restored by having $\mu \rightarrow 0$ [16–20]. In this case there can be sizable unitarity violation in neutrino propagation [34–36].

For both high- and low-scale seesaw, one can have spontaneous breaking of $U(1)_L \rightarrow \mathbb{Z}_2$, leading to the so-called majoron variants of the seesaw [17,37,38]. This is accomplished by adding the SM singlet scalar σ , which carries two units of lepton number charge. Then $\langle \sigma \rangle = v_\sigma$ spontaneously breaks $U(1)_L \rightarrow \mathbb{Z}_2$, leading to a dynamical explanation of the small neutrino masses. To get the majoron variants of minimal type-I and inverse seesaw one should replace

$$M \rightarrow Y_\sigma v_\sigma/\sqrt{2}, \quad \mu \rightarrow Y_\sigma v_\sigma/\sqrt{2} \quad (5)$$

in Eq. (1) and (3), respectively. An additional attractive feature of majoron models is the existence of a pseudo Nambu-Goldstone boson commonly dubbed as majoron. The latter carries odd charge

under \mathbb{Z}_2 thus providing a good [39–41], and testable [42,43] dark matter candidate. In the standard majoron seesaw schemes, the majoron mass is considered to be small, of order keV, for it to be a suitable warm dark matter candidate. However, the current stringent constraints on invisible Higgs boson decay modes [26,27,44,45] put severe limitation on how large $h \rightarrow \sigma\sigma$ coupling could be. On the other hand, the strength of the cosmological phase transition is expected to be strongly correlated with the size of the Higgs-majoron quartic coupling. It remains an open question whether it is possible to reconcile the current LHC bounds on the invisible Higgs decays in the inverse seesaw scenario featuring a keV-scale majoron dark matter with the existence of strong EW FOPTs yielding potentially observable GWs signals.

In this work, we consider the case where the lepton number symmetry is broken also explicitly, but softly. This way the majoron can pick up a mass. If this is larger than a half of the Standard Model (SM) Higgs boson mass, $m_h/2 \simeq 62.5$ GeV, the invisible Higgs decays will be kinematically forbidden, avoiding the stringent constraints on the Higgs-majoron quartic coupling. In such scenario the heavy majoron-like state can provide a viable candidate for cold dark matter (CDM). The same type of scalar CDM scenarios with exact \mathbb{Z}_2 parity have been broadly studied in singlet extensions of the SM [46–56], which share very similar properties with the scalar sector of the model under consideration.

2. Scalar sector

The scalar sector of the majoron inverse seesaw model has been extensively studied in the literature, including the perturbative unitarity and stability of the scalar potential, as well as the electroweak precision tests and the bounds on Higgs-majoron couplings [27,57]. The scalar potential is written as follows

$$\mathcal{V}_0(\Phi, \sigma) = \mu_\Phi^2 \Phi^\dagger \Phi + \lambda_\Phi (\Phi^\dagger \Phi)^2 + \mu_\sigma^2 \sigma^\dagger \sigma + \lambda_\sigma (\sigma^\dagger \sigma)^2 + \lambda_{\Phi\sigma} \Phi^\dagger \Phi \sigma^\dagger \sigma + \left(\frac{1}{2} \mu_b^2 \sigma^2 + \text{h.c.} \right), \quad (6)$$

with Φ and σ given by

$$\Phi = \frac{1}{\sqrt{2}} \begin{pmatrix} G + iG' \\ \phi_h + h + i\eta \end{pmatrix}, \quad \sigma = \frac{1}{\sqrt{2}} (\phi_\sigma + \sigma_R + i\sigma_I), \quad (7)$$

where h , η , G , G' , σ_R , σ_I are real scalars. These latter fields represent quantum fluctuations about the classical mean-fields $\phi_\alpha = \{\phi_h, \phi_\sigma\}$. In the zero-temperature limit, the mean-fields approach the corresponding vevs, i.e. $\phi_{h,\sigma}(T=0) \equiv v_{h,\sigma}$, where $v_h = 246$ GeV is the SM Higgs vev. Besides, one of the physical CP-even scalar states, with a small or no mixing with σ_R , is identified with the SM-like Higgs boson with mass, $m_{h_1} \equiv m_h = 125$ GeV. The last (soft) term appearing in Eq. (6) implements the explicit breakdown $U(1)_L \rightarrow \mathbb{Z}_2$, and hence provides a pseudo-Goldstone mass to the imaginary part of the field σ_I known as majoron.¹

In what follows, we discuss further implications of the majoron seesaw scenario in both versions of the scalar sector, with explicit (vanishing v_σ) and with spontaneous² ($v_\sigma \neq 0$) lepton-number $U(1)_L \rightarrow \mathbb{Z}_2$ symmetry breaking, for physics of cosmological EW FOPTs and examine the associated GWs spectra. In the first version, no mixing occurs so that

¹ One could also add other explicit breaking terms such as $\sigma \Phi^\dagger \Phi$ but here we stick to the simplest possibility of mass terms.

² More precisely, here we refer to a mixture of explicit and spontaneous $U(1)_L$ breakings in the scalar sector of the model since the soft scalar mass term $\mu_b \neq 0$ is always present in the scalar potential (6) to provide a non-zero mass to the physical majoron state. This should not be confused with the neutrino sector where $U(1)_L$ is always spontaneously broken by a small or large v_σ vev in the considered majoron versions of the seesaw schemes.

$$m_{h_1}^2 = 2\lambda_h v_h^2, \quad m_{h_2}^2 = \mu_\sigma^2 + \mu_b^2 + \frac{\lambda_{\sigma h} v_h^2}{2}, \quad (8)$$

$$m_A^2 = \mu_\sigma^2 - \mu_b^2 + \frac{\lambda_{\sigma h} v_h^2}{2}, \quad (9)$$

for the SM Higgs boson, CP-even and CP-odd (majoron) scalars, respectively. In the second version, the physical CP-even states acquire masses,

$$m_{h_1, h_2}^2 = \lambda_h v_h^2 + \lambda_\sigma v_\sigma^2 \mp \frac{\lambda_\sigma v_\sigma^2 - \lambda_h v_h^2}{\cos 2\theta}, \quad (10)$$

in terms of h - σ_R mixing angle θ , while the majoron gets a pseudo-Goldstone mass,

$$m_A^2 \equiv m_{\sigma_1}^2 = -2\mu_b^2, \quad \mu_b^2 < 0. \quad (11)$$

While in the latter case, a very light majoron (compared to the EW scale v_h) would imply setting an equally small μ_b parameter, in the former case, Eq. (9), this limit relies on a very strong fine tuning between μ_σ , μ_b and $\lambda_{\sigma h}$ model parameters. In the numerical analysis of GW spectra below we do not enforce the majoron mass m_A to be small (e.g. at a keV scale) and treat it as a free parameter instead.

3. Gravitational waves from FOPTs

In order to characterize the features of the GWs originating from FOPTs in seesaw schemes, we calculate the strength of the phase transition α at the bubble nucleation temperature T_n typically defined through the trace anomaly as [58,59]

$$\alpha = \frac{1}{\rho_\gamma} \left[V_i - V_f - \frac{T_n}{4} \left(\frac{\partial V_i}{\partial T} - \frac{\partial V_f}{\partial T} \right) \right], \quad (12)$$

with

$$\rho_\gamma = g_* \frac{\pi^2}{30} T_n^4 \quad (13)$$

being the energy density of the radiation medium at the bubble nucleation epoch found in terms of the number of relativistic d.o.f.'s. $g_* \simeq 106.75$ [60–63]. Above, V_i and V_f are the values of the effective potential in the symmetric and broken phases just before and after the transition takes place, respectively. Another key quantity to calculate the GW spectrum is the inverse time-scale β of the phase transition, which, in units of the Hubble parameter H , reads as

$$\frac{\beta}{H} = T_n \left. \frac{\partial}{\partial T} \left(\frac{\hat{S}_3}{T} \right) \right|_{T_n}, \quad (14)$$

where \hat{S}_3 is the Euclidean action. In this work, we do not consider the case of runaway bubbles and use the formalism outlined in Ref. [63] to calculate the spectrum of primordial GWs.

For the case of non-runaway nucleated bubbles, the intensity of the GW radiation grows with the ratio $\Delta v_n/T_n$, where

$$\Delta v_n^\phi = |v_\phi^f - v_\phi^i|, \quad \phi = h, \sigma \quad (15)$$

defines the difference between the VEVs of the initial (metastable) and final (stable) phases at the bubble nucleation temperature T_n . The quantity $\Delta v_n/T_n$ also offers a measure of the strength of the phase transition alternative to α . However, while the latter is of common use in the context of GWs, the former is typically referred to in the context of electroweak baryogenesis. In this work, we will consider both quantities on the same footing.

From the discussion in Ref. [59,64], it follows that bubble wall collisions do not provide an efficient way of producing GWs in the

models of interest to us here. As a result, GWs originate mainly from two sources:

- I. Magnetohydrodynamic (MHD) turbulence;
- II. Sound shock waves (SW) of the early Universe plasma, generated by the bubble's violent expansion.

These contributions arise over transient times in the early Universe and get subsequently "redshifted" by the expansion. To a present observer this appears as a cosmic gravitational stochastic background. Intuitively, one expects that from any of these leading order contributions, a high wall velocity is necessary to generate detectable GWs. In our numerical analysis, performed with the help of the CosmoTransitions package [65], we have considered supersonic detonations such that the bubble wall velocity maximizes the GW peak amplitude and is above the Chapman-Jouguet velocity defined as

$$v_J = \frac{1}{1+\alpha} \left(c_s + \sqrt{\alpha^2 + \frac{2}{3}\alpha} \right), \quad (16)$$

with $c_s = \frac{1}{\sqrt{3}}$ being the speed of sound. Besides, in our results the SW contribution dominates the peak frequency and the peak amplitude. Furthermore, the state of the art expressions derived in Ref. [63] do not account for MHD-turbulence effects due to large theoretical uncertainties. Therefore, in the remainder of this work, we will not take such effects into consideration. Note, for certain parameter configurations one also expects sequential phase transition patterns leading to multi-peak GWs spectra studied for the first time in Refs. [66,67].

3.1. Seesaw-induced GWs spectra

To investigate the eventual occurrence of phase transitions, the standard way is to incorporate into the effective potential the tree-level zero temperature components, the Coleman-Weinberg corrections, the full one-loop finite-temperature corrections, as well as the Daisy re-summation. It is worth noticing that within the type-I seesaw mechanism with explicitly broken lepton number, no FOPTs are obtained. The heavy isosinglet neutrinos practically decouple at the EW scale, and do not alter the nature of the EW phase transition. In contrast, in the non-majoron inverse seesaw mechanism (i.e. without adding a SM singlet scalar) the singlet neutrinos lie closer to the EW scale, and can have a sizable coupling to the Higgs boson. However, even by adding a large number of singlet neutrino species it is impossible to generate any sizable FOPTs at the quantum level since the fermion thermal loop contributions generate highly suppressed terms to the effective potential in the high-temperature expansion. Indeed, we find relatively weak FOPTs for many points in parameter space in this case and the corresponding GW "intensity" parameter $h^2 \Omega_{\text{GW}}^{\text{peak}}$ lies far below the sensitivity of any conceivable experiment.³

In the majoron inverse seesaw scenarios, i.e. when the scalar sector of the SM is extended by incorporating an additional complex SM-singlet scalar state, the situation changes dramatically. Indeed, it is well known that the presence of additional SM scalar singlets significantly enhances the strength and multiplicity of the FOPTs, and in some cases leads to potentially detectable GW spectra (see e.g. Refs. [68–72]). The presence of an additional classical field $\phi_\sigma \neq 0$ coupled substantially to the Higgs boson strongly affects the shape of the effective potential at non-zero temperature T allowing for a richer pattern of EW FOPTs. Note, in the considered

³ We emphasize that variations of the Yukawa coupling Y_ν in the range $1 \div 10$ cannot allow the detectability of the GW signal in the type-I seesaw scenario.

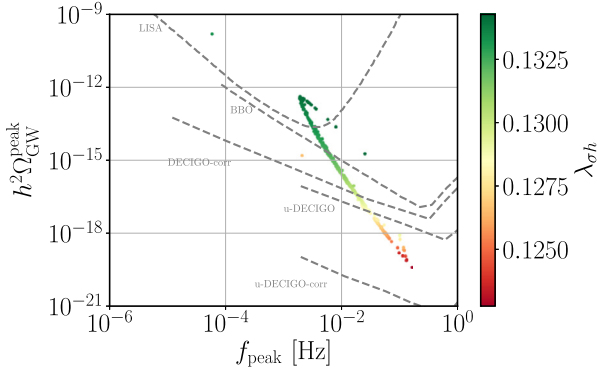


Fig. 1. The GW spectrum as a function of $\lambda_{\sigma h}$ for the case of spontaneously broken $U(1)_L$ symmetry. No solutions consistent with the LHC bound on invisibly-decaying Higgs were found. Other model parameters are fixed as: $m_A = 1$ keV, $m_{h_2} = 591$ GeV, $v_\sigma = 858$ GeV, $Y_{\sigma,1} = 1.20$, and $Y_{\sigma,2} = 1.66$ corresponding to the type-I seesaw scenario discussed in Sec. 3.3.

majoron seesaw this happens in both variants with explicit and spontaneous $U(1)_L$ breaking at $T = 0$ discussed above in Sec. 2.

The values of the coupling constants used in our numerical analysis satisfy the conservative bounds provided by tree-level perturbativity, $|\lambda_i| < 4\pi$ and $|Y_i| < \sqrt{4\pi}$, for the quartic and Yukawa couplings, respectively.⁴ Since the tree-level potential also receives both quantum and finite temperature corrections, we only considered values within the ranges $|\lambda_i| < 5$ and $|Y_i| < 3.5$, even more conservative bounds in a zero-temperature theory.

Due to the current LHC constraints on invisible Higgs decays [26,27,44,45] one has a bound $\lambda_{\sigma h} \lesssim 0.03$ the Higgs-majoron quartic coupling in the case of light keV-scale majoron. Under this assumption in our numerical scan we did not find any point with an EW FOPT that is strong enough for a potential observability of the resulting GW spectra. This is illustrated in Fig. 1.

There is a strong correlation of the peak-amplitude with $\lambda_{\sigma h}$ value such that requiring the latter to be very small makes the GW signals well below the reach of LISA or even the planned BBO and DECIGO missions. Note, this is the case for both considered versions of the majoron inverse seesaw model, with explicit and spontaneous lepton number symmetry breaking in the scalar sector at $T = 0$. Therefore, we conclude that the standard keV-scale (warm) majoron dark matter scenario associated with the inverse seesaw mechanism cannot be probed by the GW astrophysics in the current simplest formulation. For this reason, from now on we only consider the case of heavy majoron $m_A > m_h/2$ kinematically closing the invisible Higgs decay channel and thus enabling us to consider larger values of $\lambda_{\sigma h}$ that ensure the existence of the strong FOPTs in the model under consideration.

3.2. Inverse seesaw with majoron: small v_σ case

Let us now consider the case of a genuine inverse seesaw with majoron and very small singlet VEV v_σ , effectively generating an equally small μ_{SS} term in the Lagrangian (3). As discussed above, this mechanism offers a dynamical explanation for light neutrino masses, whose scale can be attributed to the (tiny) scale of spontaneous breaking of the lepton-number $U(1)_L$ symmetry in the neutrino sector (while being softly-broken in the scalar sector).

In order to understand the role of heavy neutrino in the generation of the GW spectra in the majoron inverse seesaw scenario, we study the sensitivity of the GW peak-amplitude $h^2 \Omega_{GW}^{\text{peak}}$ originated by the EW FOPTs with respect to the variation of the Yukawa

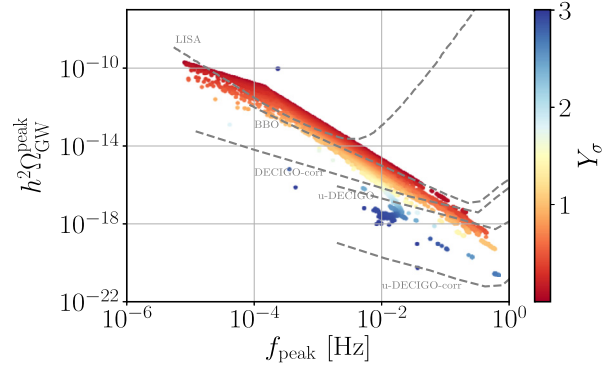


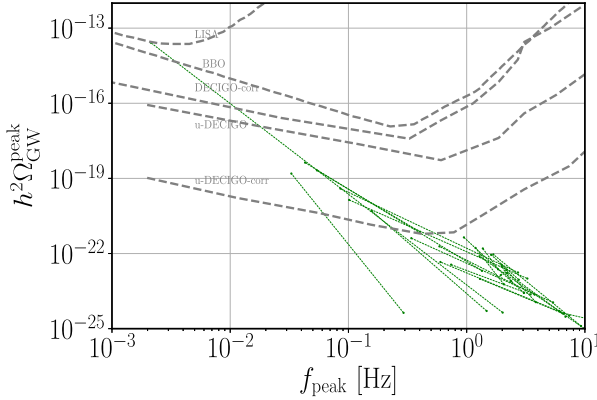
Fig. 2. The GW spectrum as a function of the Yukawa Y_σ coupling in the case of softly-broken $U(1)_L$ symmetry (i.e. $v_\sigma = 0$). Order one variation of Y_σ correspond to several order of magnitude variations in the GW power spectrum. Other model parameters are fixed as $\lambda_\sigma = 0.37$, $\lambda_{\sigma h} = 1.07$, $M = 239.4$ GeV, $m_{h_2} = 154.6$ GeV and $m_A = 369.9$ GeV.

coupling Y_σ . As shown in Fig. 2 an order one variation in the Yukawa coupling reflects into violent variations by several orders of magnitude in the GWs spectrum, with all the other parameters fixed. The results are shown together with the projected sensitivities expected in LISA, and the planned u-DECIGO and BBO missions [62,63,74,75]. We have taken the u-DECIGO sensitivity curves from Ref. [76], whereas the sensitivities of other experiments are taken from Ref. [77]. Here, for simplicity we have used the soft $U(1)_L$ breaking scenario at zero temperature, with vanishing v_σ providing a tiny value of μ in the inverse seesaw mechanism according to Eq. (5). We find a large number of points with strong FOPTs that generate the GW peak-amplitudes well within the projected LISA sensitivity, with typical values of Y_σ below unity.

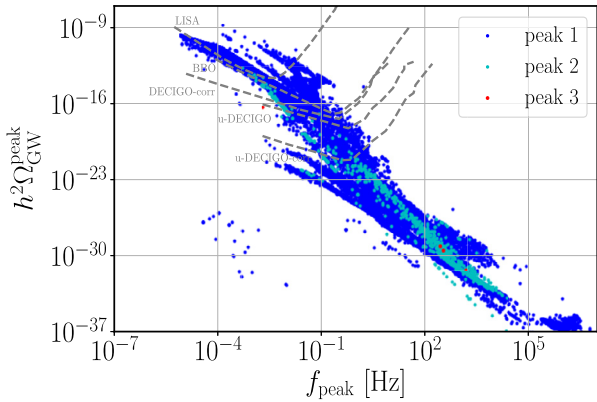
As is typical in models with several scalars, due to the presence of two classical fields $\{\phi_h, \phi_\sigma\}$ in the effective potential at finite temperatures, besides a plenty of single-step FOPTs one also finds double-step and, in some rare cases, even triple-step FOPTs for a given parameter space point and at well-separated nucleation temperatures. One could naturally expect the presence of several peaks in the corresponding GW spectrum associated with each FOPTs in such a chain of transitions. Notice also that the analyses of GW spectra for the multi-step FOPT scenarios involving EW phase transitions require particular care, as discussed for instance in Ref. [78].

Multi-peak configurations in the GW spectrum occur very frequently in the inverse seesaw with majoron. This fact is further highlighted in Fig. 3. Indeed, the double-peak feature of the GW spectrum is a generic prediction of our model, that can arise for many parameter choices, as shown in Fig. 3a. Configurations with larger peak multiplicities are also possible, as seen in Fig. 3b, where the color denotes the peak number, 1 (blue), 2 (cyan) or 3 (red). Such a rich structure of the GW spectrum is favoured for relatively large quartic couplings involving σ . From Fig. 3b we also see that the GW spectra with three peaks are rarer than single or double GW-peak spectra. We also note that a significant fraction of the single peak cases are potentially testable at LISA and BBO. However, finding a well-resolved double- or triple-peak feature where more than a single peak could be observable in a measurement appears to be very challenging. No single point with such a feature has been found by our scans. As seen in Fig. 3a in most cases both peak-amplitudes occur below the projected sensitivities of any planned measurements rendering the observability of the corresponding scenarios very remote. In a subset of cases, only the largest peak has been found in the sensitivity ranges of the planned BBO and u-DECIGO missions, while the second peak typically lies outside of the reach of future detectors. This is a direct consequence of the not-so-large quartic couplings that are restricted to be smaller than five. While larger values of the quartic

⁴ For a more involved analysis of the perturbativity constraints in a scalar extension of the SM, see e.g. Ref. [73].



(a) Selected double-peak scenarios within the LISA and BBO sensitivity ranges. The two ends of each line represent the location of the peaks of the double-peak GW spectrum. The two maxima in each double-peak GW spectra are joined by a straight line, in order to easily identify the peaks associated with each other.



(b) Scatter plot showing the number of peaks for given model parameter choices. Notice the appearance of double- and even triple-peak features.

Fig. 3. The multi-peak feature arising from different phase transitions in the cosmological history of the Universe is very generic in the inverse seesaw with majoron.

tic couplings could generate well-separate and measurable double-peak signatures, these scenarios may suffer from larger underlined theoretical uncertainties so we decided not to discuss them here.

In order to understand the characteristic features of the GW spectra in the majoron inverse seesaw, in Fig. 4 we show the GW energy density spectrum obtained for distinct nucleation temperatures T_n . Here, we have depicted three benchmark scenarios (for the case of vanishing v_σ) originating from the single-step FOPT (green line) as well as double-step FOPTs i.e. with two consecutive strong phase transitions (red and blue lines). The corresponding values for the model parameters are given in Table 1 and Table 2.

The green curve represents a single-peak scenario with a very strong $U(1)_L$ phase transition, $\Delta v_\sigma(T_n)/T_n \simeq 10$, and softly-broken lepton symmetry. It features a very strong FOPT but not EW one. In fact, this peak is a probe of $U(1)_L$ breaking at finite temperatures while the associated EWPT is very weak or even of second order. This is possible due to relatively large values of a quartic (portal) coupling, $\lambda_{\sigma h} \simeq 2$, and majoron-neutrino Yukawa coupling, $Y_\sigma \simeq 2$, which make the m/T -ratio sizable. Hence, the cubic (m/T)³ terms in the thermal expansion can produce a potential barrier between both vacua, inducing this type of transitions.

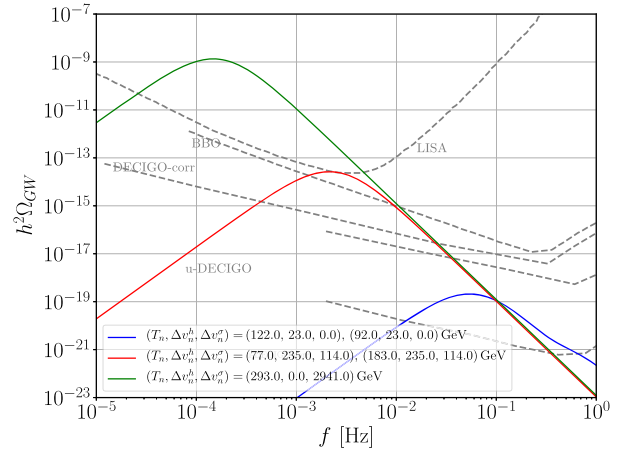


Fig. 4. Inverse-seesaw-with-majoron benchmark GW spectra in the scenario with soft $U(1)_L$ symmetry breaking (i.e. with vanishingly small $v_\sigma(T=0) \rightarrow 0$). The green curve represents the case with single-step FOPT, while the blue and red curves correspond to double-step FOPTs whose characteristics are given in Tables 1 and 2. For double-step transitions, the (T_n, v_n) pairs in each peak are ordered from low to high frequencies. Here, $\Delta v_h^h = |v_h^f - v_h^i|$ and $\Delta v_\sigma^\sigma = |v_\sigma^f - v_\sigma^i|$ at a given nucleation temperature $T = T_n$.

Table 1

Phase transition parameters for the three curves in Fig. 4. In “peak Id” column, the numbering of multi-step scenarios is ordered from high to low nucleation temperature T_n , given in units of GeV. The vevs before the transition ($v_{h,\sigma}^i$) and after the transition ($v_{h,\sigma}^f$) are given in units of GeV.

Peak Id	T_n	$(v_h^i, v_\sigma^i) \rightarrow (v_h^f, v_\sigma^f)$	α	β/H
Green 1	293	$(0, 0) \rightarrow (0, 2941)$	0.5	4.9
Red 1	183	$(0, 114) \rightarrow (235, 0)$	7.7×10^{-4}	7.2×10^4
Red 2	77	$(0, 114) \rightarrow (235, 0)$	0.1	231
Blue 1	122	$(193, 0) \rightarrow (216, 0)$	1.4×10^{-2}	3.1×10^3
Blue 2	92	$(193, 0) \rightarrow (216, 0)$	9.4×10^{-3}	3.0×10^4

Table 2

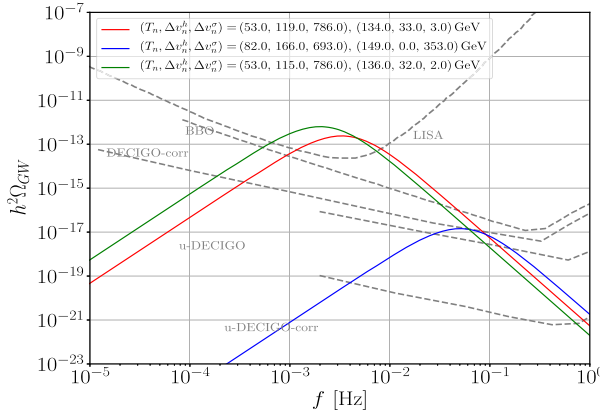
Model parameters for the three curves in Fig. 4. Mass parameters are given in units of GeV.

Curve	m_{h_2}	m_A	$\lambda_{\sigma h}$	λ_σ	M	Y_σ
Green	236	708	1.7	5×10^{-3}	380	2
Red	192	970	2.3	1.5	93	0.1
Blue	325	169	4	2.7	158	0.1

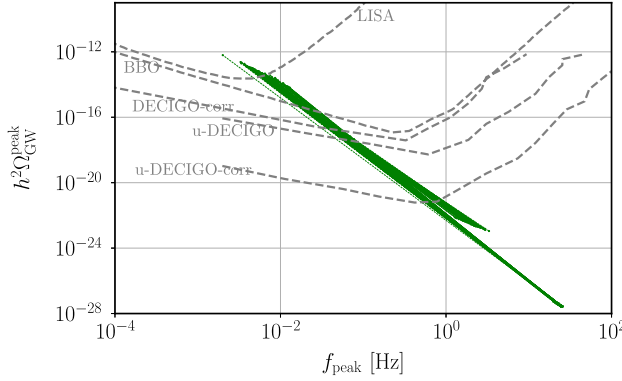
On another hand, the other two benchmark points, which have the double-peak feature, have strong EWPT for both peaks in the red curve and for the smaller, almost invisible, peak of the blue curve. Besides this, the blue curve has no $U(1)_L$ breaking in any of the minima of the effective potential at the corresponding nucleation temperatures whereas the red curve exhibits a strong $U(1)_L$ breaking for the higher peak and a weak $U(1)_L$ breaking for the hidden peak. Similarly to the single-peak scenario, the observable peaks in the red and blue curves are generated due to large $\lambda_{\sigma h}$ and λ_σ couplings. Note, the single-peak case (green line) lies well within the LISA range [62,63,74], while only the largest peaks in the double-step FOPT scenarios are within the planned sensitivity range of the BBO (red line) and u-DECIGO-corr (blue line) measurements [75], respectively.

3.3. Type-I seesaw with majoron: large v_σ

To further illustrate the importance of future GW measurements for probing neutrino mass generation mechanisms let us consider a type-I seesaw with majoron where the heavy neutrino



(a) The expected GW spectra.



(b) Scatter plot showing typical double-peak scenarios.

Fig. 5. Gravitational footprints of “fake” low-scale seesaw with majoron. In both plots we take $v_\sigma \sim \mathcal{O}(100)$ GeV – $\mathcal{O}(1)$ TeV.

mass scale M is generated via a large majoron vev v_σ spontaneously breaking the lepton number symmetry.

As mentioned above, it is clear that, if $Y_\nu \sim \mathcal{O}(1)$, then $M = Y_\nu v_\sigma / \sqrt{2} \sim \mathcal{O}(10^{14})$ GeV, hence $v_\sigma \sim \mathcal{O}(10^{14})$ GeV for $Y_\sigma \sim \mathcal{O}(1)$. In this limit, all the new particles can be integrated out for processes occurring at the EW scale,⁵ leading to no-FOPT solutions.

However, one can take $Y_\nu \sim \mathcal{O}(10^{-6})$, corresponding to $M = Y_\nu v_\sigma / \sqrt{2} \sim \mathcal{O}(100)$ GeV. The majoron and neutrino fields do not decouple at the EW scale in this case, and can still lead to strong FOPTs – hence to potentially observable primordial GW signals. One sees that this “fake” low-scale seesaw scenario requires tiny values of the neutrino “Dirac” Yukawa couplings Y_ν to fit the small neutrino masses in the presence of relatively large $U(1)_L$ symmetry breaking scale v_σ that can be placed not too far from the EW scale. Such “fake” low-scale seesaw contrasts with the “genuine” low-scale seesaw considered in Sec. 3.2, which does not require this restriction.

Here, for an easy one-to-one comparison with the “genuine” inverse seesaw scenario studied above, we will consider a type-I majoron seesaw model with six heavy neutrinos. This way we preserve the number of fermionic degrees of freedom entering the thermal corrections by considering the following Lagrangian

$$\mathcal{L}_{\text{Yuk}}^{\text{Type-I}} = Y_{\nu,i} \bar{L} H v_i^c + Y_{\sigma,i} \sigma v_i^c v_i^c + h.c. \quad (17)$$

where v^c and S in the inverse seesaw scenario are replaced by v_1^c and v_2^c in this extended type-I seesaw variant, and the off-diagonal

Table 3

FOPT parameters for the three curves in Fig. 5a. The vevs before ($v_{h,\sigma}^i$) and after ($v_{h,\sigma}^f$) the phase transition are given in units of GeV.

Peak Id	T_n	$(v_{h,\sigma}^i, v_{\sigma}^i) \rightarrow (v_{h,\sigma}^f, v_{\sigma}^f)$	α	β/H
Green 1	136	$(0, 921) \rightarrow (32, 919)$	9.4×10^{-5}	1.2×10^6
Green 2	53	$(245, 786) \rightarrow (360, 0)$	0.5	378
Red 1	134	$(0, 922) \rightarrow (33, 919)$	10^{-4}	1.1×10^6
Red 2	53	$(245, 786) \rightarrow (364, 0)$	0.5	612
Blue 1	149	$(0, 353) \rightarrow (0, 0)$	1.5×10^{-3}	1.0×10^5
Blue 2	82	$(205, 693) \rightarrow (40, 0)$	0.03	4.9×10^3

Table 4

Model parameters for the three curves in Fig. 5a. Masses and v_σ are given in units of GeV.

Curve	m_{h_2}	m_A	λ_h	$\lambda_{\sigma h}$	λ_σ	θ	v_σ	$Y_{\sigma,1}$	$Y_{\sigma,2}$
Green	203	188	0.14	0.03	0.03	0.26	790	0.07	1.58
Red	206	188	0.14	0.03	0.03	0.26	790	0.08	1.59
Blue	205	188	0.14	-0.02	0.03	-0.18	790	0.08	1.59

terms in the heavy neutrino mass matrix and “Dirac” Yukawa couplings $Y_{\nu,i}$ are assumed to be negligibly small. As our main result, we find that, in a large region of parameter space, both “fake” and “genuine” low-scale seesaw + majoron lead to the possibility of strong FOPTs. The corresponding GW spectra in the “fake” seesaw obtained for $v_\sigma \sim \mathcal{O}(100)$ GeV – $\mathcal{O}(1)$ TeV are shown in Fig. 5. Parameter values of this model associated to Fig. 5a are given in Table 4 and Table 3.

4. Conclusion

To conclude, we analysed the most popular implementations of the type-I seesaw mechanism for neutrino mass generation. We studied both the cases of explicit and spontaneous breakdown of the lepton number symmetry in the neutrino sector. The second, “dynamical” symmetry breaking implies the majoron field. We have found that various scenarios lead to different patterns of phase transitions. We showed that explicit lepton number violation in the neutrino sector cannot induce any strong electroweak phase transition. Therefore, it does not lead to any gravitational-wave background signal testable by next-generation satellite interferometers.

The case when neutrino masses emerge from a dynamical mechanism in which lepton number violation happens spontaneously leads to much clearer gravitational footprints. Within such majoron seesaw case, we found that both the standard type-I seesaw (taken at a low scale) and the “genuine” low-scale type-I seesaw (like the inverse seesaw) predict a strong gravitational wave signal, testable in the 0.1 – 100 mHz frequency range. This highly motivates future experimental proposals, including LISA, u-DECIGO and BBO missions, accessing to the mHz frontier, as an indirect and complementary probe of neutrino mass generation, providing an important information on the electroweak phase transition.

While “genuine” low-scale seesaw would also predict large charged lepton flavor violation [29–33], and unitarity violation in neutrino propagation [34–36], these features are absent in the “fake” low-scale seesaw. This way one can distinguish the two schemes in high-intensity/energy frontier setups. Here we have shown that “fake” and “genuine” schemes may also have potentially distinct gravitational footprints. We saw explicitly that they can produce different gravitational-wave spectra, testable in upcoming gravitational-wave experiments. As we stand right now, the new portal provided by the gravitational-wave physics in the multi-messenger era may contribute to shed light on the mystery of neutrino mass generation.

⁵ All the physical majoron couplings are highly suppressed yielding no effect on EW scale physics.

Declaration of competing interest

The authors declare that they have no known competing financial interests or personal relationships that could have appeared to influence the work reported in this paper.

Acknowledgements

Useful discussions and correspondence with Zurab Berezhiani, Yifu Cai and Nico Yunes are gratefully acknowledged. A.P.M. wants to thank Marek Lewicki and Bogumiła Świeżewska for insightful discussions about bubble wall collision contributions to the spectrum of GW. A.A. and A.M. wish to acknowledge support by the NSFC, through grant No. 11875113, the Shanghai Municipality, through grant No. KBH1512299, and by Fudan University, through grant No. JJJH1512105. J.B. acknowledges his partial support by the NSFC, through the grants No. 11375153 and 11675145. A.A. and A.M. would like to thank IFIC for hospitality during the preparation of this work. R.P. is supported in part by the Swedish Research Council grants, contract numbers 621-2013-4287 and 2016-05996, as well as by the European Research Council (ERC) under the European Union's Horizon 2020 research and innovation programme (grant agreement No 668679). The work of R.P. was also supported in part by The Ministry of Education, Youth and Sports of the Czech Republic, project LT17018. The work of A.P.M. has been performed in the framework of COST Action CA16201 "Unraveling new physics at the LHC through the precision frontier" (PARTICLEFACE). A.P.M. is supported by the Center for Research and Development in Mathematics and Applications (CIDMA) through the Portuguese Foundation for Science and Technology (FCT - Fundação para a Ciência e a Tecnologia), references UIDB/04106/2020 and UIDP/04106/2020 and by national funds (OE), through FCT, I.P., in the scope of the framework contract foreseen in the numbers 4, 5 and 6 of the article 23, of the Decree-Law 57/2016, of August 29, changed by Law 57/2017, of July 19. A.P.M. is also supported by the *Enabling Green E-science for the Square Kilometer Array Research Infrastructure* (ENGAGESKA), POCI-01-0145-FEDER-022217, and by the projects PTDC/FIS-PAR/31000/2017 and CERN/FIS-PAR/0027/2019. R.V. and J.W.F.V. are supported by the Spanish grants SEV-2014-0398 and FPA2017-85216-P (AEI/FEDER, UE), PROMETEO/2018/165 (Generalitat Valenciana) and the Spanish Red Consolider MultiDark FPA2017-90566-REDT.

References

- [1] T. Kajita, Nobel lecture: discovery of atmospheric neutrino oscillations, Rev. Mod. Phys. 88 (2016) 030501.
- [2] A.B. McDonald, Nobel lecture: the Sudbury neutrino observatory: observation of flavor change for solar neutrinos, Rev. Mod. Phys. 88 (2016) 030502.
- [3] J.W.F. Valle, J.C. Romao, Neutrinos in High Energy and Astroparticle Physics, John Wiley & Sons, 2015, www.wiley.com/buy/9783527411979.
- [4] S. Weinberg, Varieties of baryon and lepton nonconservation, Phys. Rev. D 22 (1964).
- [5] S.M. Boucenna, S. Morisi, J.W.F. Valle, The low-scale approach to neutrino masses, Adv. High Energy Phys. 2014 (2014) 831598, arXiv:1404.3751 [hep-ph].
- [6] E. Ma, R. Srivastava, Dirac or inverse seesaw neutrino masses with $B - L$ gauge symmetry and S_3 flavor symmetry, Phys. Lett. B 741 (2015) 217–222, arXiv: 1411.5042 [hep-ph].
- [7] E. Ma, N. Pollard, R. Srivastava, M. Zakeri, Gauge $B - L$ model with residual Z_3 symmetry, Phys. Lett. B 750 (2015) 135–138, arXiv:1507.03943 [hep-ph].
- [8] S. Centelles Chuliá, et al., Dirac neutrinos and dark matter stability from lepton quarticity, Phys. Lett. B 767 (2017) 209–213, arXiv:1606.04543 [hep-ph].
- [9] S. Centelles Chuliá, R. Srivastava, J.W.F. Valle, Seesaw roadmap to neutrino mass and dark matter, Phys. Lett. B 781 (2018) 122–128, arXiv:1802.05722 [hep-ph].
- [10] S. Centelles Chuliá, R. Srivastava, J.W.F. Valle, Seesaw Dirac neutrino mass through dimension-six operators, Phys. Rev. D 98 (3) (2018) 035009, arXiv: 1804.03181 [hep-ph].
- [11] C. Bonilla, S. Centelles Chuliá, R. Cepedello, E. Peinado, R. Srivastava, Dark matter stability and Dirac neutrinos using only standard model symmetries, arXiv:1812.01599 [hep-ph].
- [12] P. Minkowski, $\mu \rightarrow e\gamma$ at a rate of one out of 1-billion muon decays?, Phys. Lett. B 67 (1977) 421.
- [13] T. Yanagida, Horizontal symmetry and masses of neutrinos, in: O. Sawada, A. Sugamoto (Eds.), Workshop on the Baryon Number of the Universe and Unified Theories, 1979, p. 95.
- [14] R.N. Mohapatra, G. Senjanovic, Neutrino mass and spontaneous parity violation, Phys. Rev. Lett. 44 (1980) 912.
- [15] J. Schechter, J.W.F. Valle, Neutrino masses in $SU(2) \times U(1)$ theories, Phys. Rev. D 22 (1980) 2227.
- [16] R. Mohapatra, J.W.F. Valle, Neutrino mass and baryon number nonconservation in superstring models D34 (1986) 1642.
- [17] M. Gonzalez-Garcia, J.W.F. Valle, Fast decaying neutrinos and observable flavor violation in a new class of majoron models, Phys. Lett. B 216 (1989) 360–366.
- [18] E.K. Akhmedov, et al., Left-right symmetry breaking in NJL approach, Phys. Lett. B 368 (1996) 270–280, arXiv:hep-ph/9507275 [hep-ph].
- [19] E.K. Akhmedov, et al., Dynamical left-right symmetry breaking, Phys. Rev. D 53 (1996) 2752–2780, arXiv:hep-ph/9509255 [hep-ph].
- [20] M. Malinsky, J. Romao, J.W.F. Valle, Novel supersymmetric $SO(10)$ seesaw mechanism, Phys. Rev. Lett. 95 (2005) 161801, arXiv:hep-ph/0506296 [hep-ph].
- [21] S. Das, et al., Heavy neutrinos and lepton flavour violation in left-right symmetric models at the LHC, Phys. Rev. D 86 (2012) 055006, arXiv:1206.0256 [hep-ph].
- [22] F.F. Deppisch, N. Desai, J.W.F. Valle, Is charged lepton flavor violation a high energy phenomenon?, Phys. Rev. D 89 (2014) 051302, arXiv:1308.6789 [hep-ph].
- [23] F.F. Deppisch, P. Bhupal Dev, A. Pilaftsis, Neutrinos and collider physics, New J. Phys. 17 (2015) 075019, arXiv:1502.06541 [hep-ph].
- [24] A.S. Joshipura, J.W.F. Valle, Invisible Higgs decays and neutrino physics, Nucl. Phys. B 397 (1) (1993) 105–122, <http://www.sciencedirect.com/science/article/pii/0550321393903370>.
- [25] M.A. Diaz, et al., Seesaw majoron model of neutrino mass and novel signals in Higgs boson production at LEP, Nucl. Phys. B 527 (1998) 44–60, arXiv:hep-ph/9803362 [hep-ph].
- [26] C. Bonilla, J.C. Romao, J.W.F. Valle, Electroweak breaking and neutrino mass: invisible Higgs decays at the LHC (type II seesaw), New J. Phys. 18 (3) (2016) 033033, arXiv:1511.07351 [hep-ph].
- [27] C. Bonilla, J.W.F. Valle, J.C. Romao, Neutrino mass and invisible Higgs decays at the LHC, Phys. Rev. D 91 (11) (2015) 113015, arXiv:1502.01649 [hep-ph].
- [28] A. Kosowsky, M.S. Turner, R. Watkins, Gravitational waves from first order cosmological phase transitions, Phys. Rev. Lett. 69 (1992) 2026–2029.
- [29] J. Bernabeu, et al., Lepton flavor nonconservation at high-energies in a superstring inspired standard model, Phys. Lett. B 187 (1987) 303.
- [30] G.C. Branco, M.N. Rebelo, J.W.F. Valle, Leptonic CP violation with massless neutrinos, Phys. Lett. B 225 (1989) 385–392.
- [31] N. Rius, J.W.F. Valle, Leptonic CP violating asymmetries in Z^0 decays, Phys. Lett. B 246 (1990) 249–255.
- [32] F. Deppisch, J.W.F. Valle, Enhanced lepton flavor violation in the supersymmetric inverse seesaw model, Phys. Rev. D 72 (2005) 036001, arXiv:hep-ph/0406040 [hep-ph].
- [33] S. Antusch, C. Biggio, E. Fernandez-Martinez, M. Gavela, J. Lopez-Pavon, Unitarity of the leptonic mixing matrix, J. High Energy Phys. 0610 (2006) 084.
- [34] F. Escrivuela, et al., On the description of nonunitary neutrino mixing, Phys. Rev. D 92 (2015) 053009, arXiv:1503.08879 [hep-ph].
- [35] D. Forero, et al., Lepton flavor violation and non-unitary lepton mixing in low-scale type-I seesaw, J. High Energy Phys. 1109 (2011) 142, arXiv:1107.6009 [hep-ph].
- [36] O. Miranda, M. Tortola, J.W.F. Valle, New ambiguity in probing CP violation in neutrino oscillations, Phys. Rev. Lett. 117 (2016) 061804, arXiv:1604.05690 [hep-ph].
- [37] Y. Chikashige, R.N. Mohapatra, R.D. Peccei, Are there real Goldstone bosons associated with broken lepton number?, Phys. Lett. B 98 (1981) 265–268.
- [38] J. Schechter, J.W.F. Valle, Neutrino decay and spontaneous violation of lepton number, Phys. Rev. D 25 (1982) 774.
- [39] V. Berezinsky, J.W.F. Valle, The KeV majoron as a dark matter particle, Phys. Lett. B 318 (1993) 360–366, arXiv:hep-ph/9309214 [hep-ph].
- [40] M. Lattanzi, J.W.F. Valle, Decaying warm dark matter and neutrino masses, Phys. Rev. Lett. 99 (2007) 121301, arXiv:0705.2406 [astro-ph].
- [41] J.-L. Kuo, et al., Decaying warm dark matter and structure formation, J. Cosmol. Astropart. Phys. 1812 (12) (2018) 026, arXiv:1803.05650 [astro-ph.CO].
- [42] M. Lattanzi, et al., Updated CMB, X- and gamma-ray constraints on majoron dark matter, Phys. Rev. D 88 (2013) 063528, arXiv:1303.4685 [astro-ph.HE].
- [43] F. Bazzocchi, et al., X-ray photons from late-decaying majoron dark matter, J. Cosmol. Astropart. Phys. 0808 (2008) 013, arXiv:0805.2372 [astro-ph].
- [44] ATLAS Collaboration, M. Aaboud, et al., Search for invisible Higgs boson decays in vector boson fusion at $\sqrt{s} = 13$ TeV with the ATLAS detector, Phys. Lett. B 793 (2019) 499–519, arXiv:1809.06682 [hep-ex].
- [45] CMS Collaboration, A.M. Sirunyan, et al., Search for invisible decays of a Higgs boson produced through vector boson fusion in proton-proton collisions at $\sqrt{s} = 13$ TeV, Phys. Lett. B 793 (2019) 520–551, arXiv:1809.05937 [hep-ex].

- [46] R. Costa, A.P. Morais, M.O.P. Sampaio, R. Santos, Two-loop stability of a complex singlet extended standard model, *Phys. Rev. D* 92 (2015) 025024, arXiv:1411.4048 [hep-ph].
- [47] C. Burgess, M. Pospelov, T. ter Veldhuis, The minimal model of nonbaryonic dark matter: a singlet scalar, *Nucl. Phys. B* 619 (2001) 709–728, arXiv:hep-ph/0011335.
- [48] M. Gonderinger, H. Lim, M.J. Ramsey-Musolf, Complex scalar singlet dark matter: vacuum stability and phenomenology, *Phys. Rev. D* 86 (2012) 043511, arXiv:1202.1316 [hep-ph].
- [49] J.M. Cline, K. Kainulainen, P. Scott, C. Weniger, Update on scalar singlet dark matter, *Phys. Rev. D* 88 (2013) 055025, arXiv:1306.4710 [hep-ph]; Erratum: *Phys. Rev. D* 92 (2015) 039906.
- [50] E. Gabrielli, M. Heikinheimo, K. Kannike, A. Racioppi, M. Raidal, C. Spethmann, Towards completing the standard model: vacuum stability, EWSB and dark matter, *Phys. Rev. D* 89 (1) (2014) 015017, arXiv:1309.6632 [hep-ph].
- [51] N. Khan, S. Rakshit, Study of electroweak vacuum metastability with a singlet scalar dark matter, *Phys. Rev. D* 90 (11) (2014) 113008, arXiv:1407.6015 [hep-ph].
- [52] K. Ghorbani, P.H. Ghorbani, A simultaneous study of dark matter and phase transition: two-scalar scenario, *J. High Energy Phys.* 12 (2019) 077, arXiv:1906.01823 [hep-ph].
- [53] C. Cosme, J.G. Rosa, O. Bertolami, Can dark matter drive electroweak symmetry breaking?, arXiv:1811.08908 [hep-ph].
- [54] D. Azevedo, M. Duch, B. Grzadkowski, D. Huang, M. Iglicki, R. Santos, Testing scalar versus vector dark matter, *Phys. Rev. D* 99 (1) (2019) 015017, arXiv:1808.01598 [hep-ph].
- [55] B. Grzadkowski, D. Huang, Spontaneous CP-violating electroweak baryogenesis and dark matter from a complex singlet scalar, *J. High Energy Phys.* 08 (2018) 135, arXiv:1807.06987 [hep-ph].
- [56] C.-W. Chiang, M.J. Ramsey-Musolf, E. Senaha, Standard model with a complex scalar singlet: cosmological implications and theoretical considerations, *Phys. Rev. D* 97 (1) (2018) 015005, arXiv:1707.09960 [hep-ph].
- [57] T. Brune, H. Päs, Massive majorons and constraints on the majoron-neutrino coupling, *Phys. Rev. D* 99 (2019) 096005, arXiv:1808.08158 [hep-ph].
- [58] M. Hindmarsh, S.J. Huber, K. Rummukainen, D.J. Weir, Numerical simulations of acoustically generated gravitational waves at a first order phase transition, *Phys. Rev. D* 92 (12) (2015) 123009, arXiv:1504.03291 [astro-ph.CO].
- [59] M. Hindmarsh, S.J. Huber, K. Rummukainen, D.J. Weir, Shape of the acoustic gravitational wave power spectrum from a first order phase transition, *Phys. Rev. D* 96 (10) (2017) 103520, arXiv:1704.05871 [astro-ph.CO].
- [60] C. Grojean, G. Servant, Gravitational waves from phase transitions at the electroweak scale and beyond, *Phys. Rev. D* 75 (2007) 043507, arXiv:hep-ph/0607107 [hep-ph].
- [61] L. Leitao, A. Megevand, Gravitational waves from a very strong electroweak phase transition, *J. Cosmol. Astropart. Phys.* 1605 (05) (2016) 037, arXiv:1512.08962 [astro-ph.CO].
- [62] C. Caprini, et al., Science with the space-based interferometer eLISA. II: Gravitational waves from cosmological phase transitions, *J. Cosmol. Astropart. Phys.* 1604 (04) (2016) 001, arXiv:1512.06239 [astro-ph.CO].
- [63] C. Caprini, et al., Detecting gravitational waves from cosmological phase transitions with LISA: an update, *J. Cosmol. Astropart. Phys.* 2003 (03) (2020) 024, arXiv:1910.13125 [astro-ph.CO].
- [64] J. Ellis, M. Lewicki, J.M. No, V. Vaskonen, Gravitational wave energy budget in strongly supercooled phase transitions, *J. Cosmol. Astropart. Phys.* 1906 (06) (2019) 024, arXiv:1903.09642 [hep-ph].
- [65] C.L. Wainwright, CosmoTransitions: computing cosmological phase transition temperatures and bubble profiles with multiple fields, *Comput. Phys. Commun.* 183 (2012) 2006–2013, arXiv:1109.4189 [hep-ph].
- [66] T. Vieu, A.P. Morais, R. Pasechnik, Multi-peaked signatures of primordial gravitational waves from multi-step electroweak phase transition, arXiv:1802.10109 [hep-ph].
- [67] A.P. Morais, R. Pasechnik, Probing multi-step electroweak phase transition with multi-peaked primordial gravitational waves spectra, arXiv:1910.00717 [hep-ph].
- [68] K. Hashino, R. Jinno, M. Kakizaki, S. Kanemura, T. Takahashi, M. Takimoto, Selecting models of first-order phase transitions using the synergy between collider and gravitational-wave experiments, *Phys. Rev. D* 99 (7) (2019) 075011, arXiv:1809.04994 [hep-ph].
- [69] A. Alves, T. Ghosh, H.-K. Guo, K. Sinha, D. Vagie, Collider and gravitational wave complementarity in exploring the singlet extension of the standard model, *J. High Energy Phys.* 04 (2019) 052, arXiv:1812.09333 [hep-ph].
- [70] G. Kurup, M. Perelstein, Dynamics of electroweak phase transition in singlet-scalar extension of the standard model, *Phys. Rev. D* 96 (1) (2017) 015036, arXiv:1704.03381 [hep-ph].
- [71] K. Hashino, M. Kakizaki, S. Kanemura, P. Ko, T. Matsui, Gravitational waves and Higgs boson couplings for exploring first order phase transition in the model with a singlet scalar field, *Phys. Lett. B* 766 (2017) 49–54, arXiv:1609.00297 [hep-ph].
- [72] M. Kakizaki, S. Kanemura, T. Matsui, Gravitational waves as a probe of extended scalar sectors with the first order electroweak phase transition, *Phys. Rev. D* 92 (11) (2015) 115007, arXiv:1509.08394 [hep-ph].
- [73] S. Moretti, K. Yagyu, Constraints on parameter space from perturbative unitarity in models with three scalar doublets, *Phys. Rev. D* 91 (2015) 055022, arXiv:1501.06544 [hep-ph].
- [74] LISA Collaboration, P. Amaro-Seoane, et al., Laser interferometer space antenna, arXiv:1702.00786 [astro-ph.IM].
- [75] H. Kudoh, A. Taruya, T. Hiramatsu, Y. Himemoto, Detecting a gravitational-wave background with next-generation space interferometers, *Phys. Rev. D* 73 (2006) 064006, arXiv:gr-qc/0511145 [gr-qc].
- [76] K. Nakayama, J. Yokoyama, Gravitational wave background and non-Gaussianity as a probe of the curvaton scenario, *J. Cosmol. Astropart. Phys.* 1001 (2010) 010, arXiv:0910.0715 [astro-ph.CO].
- [77] C.J. Moore, R.H. Cole, C.P.L. Berry, Gravitational-wave sensitivity curves, *Class. Quantum Gravity* 32 (1) (2015) 015014, arXiv:1408.0740 [gr-qc].
- [78] J. Ellis, M. Lewicki, J.M. No, On the maximal strength of a first-order electroweak phase transition and its gravitational wave signal, arXiv:1809.08242 [hep-ph].